

Supporting Information

5-(Dinitromethyl)-3-(trinitromethyl)-1,2,4-triazole and Its Derivatives: A New Application of Oxidative Nitration Towards *Gem*-trinitro-based Energetic Materials

Srinivas Dharavath,^a Jiaheng Zhang,^{*b} Gregory H. Imler,^c Damon A. Parrish,^c and Jean'ne M. Shreeve^{*a}

^aDepartment of Chemistry, University of Idaho, Moscow, Idaho 83844-2343, USA. E-mail: jshreeve@uidaho.edu

^bSchool of Materials Science and Engineering, Harbin Institute of Technology, Shenzhen, 518055, China. E-mail: jzhang@uidaho.edu

^cNaval Research Laboratory, 4555 Overlook Avenue, Washington, D.C. 20375, USA

Table of Contents

1. ¹⁵ N Spectra of 6 and 8	
Figures S1 and S2	S2
3. X-ray Crystallography of 8	S3-S7
Table S1	S3-S4
Figures S3 to S6	S4-S6
Tables S2	S7
4. Theoretical calculations	S7-S11
5. References	S11-S12

In Figures S1 and S2, ^{15}N NMR spectra of **6** and **8** are given. The assignments are based on the literature values of resonance peaks in similar compounds^[1,2] and compared with calculated spectra [B3LYP/6-311+g(2d,p) with IEF-PCM continuum solvation models of the Gaussian 03 program].^[3,4]

Compound 6

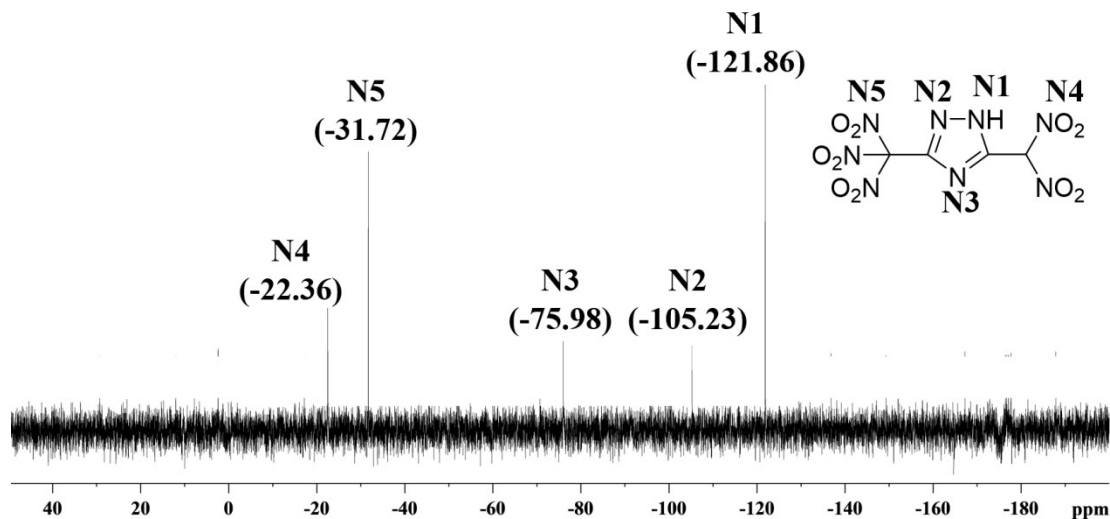


Figure S1. ^{15}N spectrum of **6** in DMSO- d_6 .

Compound 8

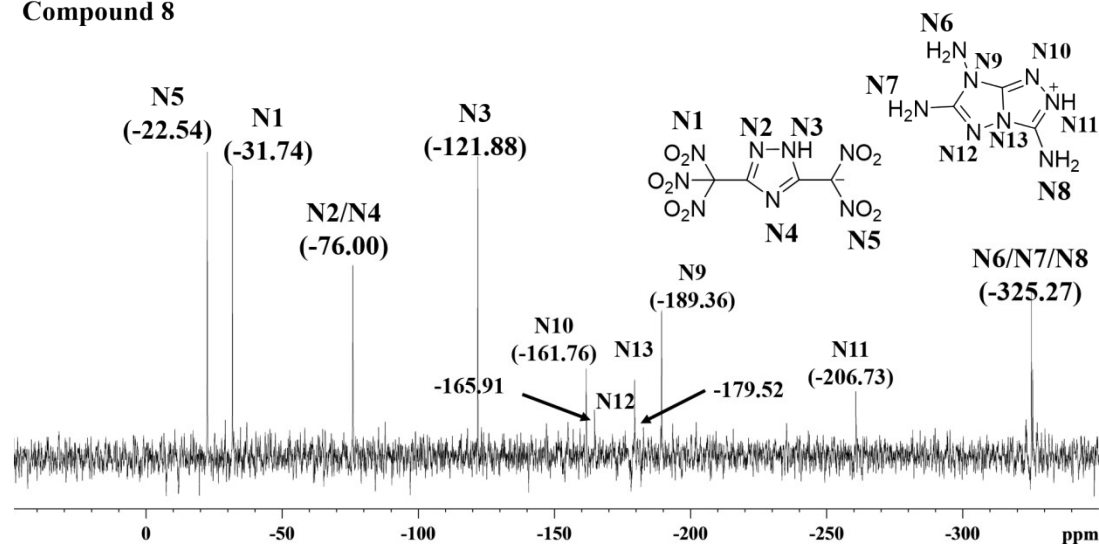


Figure S2. ^{15}N spectrum of **8** in DMSO- d_6 .

X-ray Crystallography of **8**

An orange crystal of dimensions 0.431 x 0.190 x 0.040 mm³ was mounted on a MiteGen MicroMesh using a small amount of Cargille immersion oil. Data were collected on a Bruker three-circle platform diffractometer equipped with a SMART APEX II CCD detector. The crystals were irradiated using graphite monochromated MoK_α radiation ($\lambda = 0.71073$). An Oxford Cobra low temperature device was used to maintain the crystals at a constant 150(2) K during data collection.

Data collection was performed and the unit cell was initially refined using *APEX2* [v2014.3-0].^[5] Data reduction was performed using *SAINTE* [v7.68A]^[6] and *XPREF* [v2014/2].^[7] Corrections were applied for Lorentz, polarization, and absorption effects using *SADABS* [v2008/1].^[8] The structure was solved and refined with the aid of the programs SHELXL-2014/7 within WingX.^[9] The full-matrix least-squares refinement on F² included atomic coordinates and anisotropic thermal parameters for all non-H atoms. The H atoms were included using a riding model (Table S1).

Table S1. Selected crystal parameters of **8**

Empirical formula	C ₇ H ₈ N ₁₆ O ₁₀
	(8)
Formula weight	476.29
Temperature/K	150
Crystal system	monoclinic
Space group	P2 ₁ /c
a/Å	12.337(2)
b/Å	11.4124(19)
c/Å	11.8204(19)
α /°	90
β /°	100.961(6)
γ /°	90

Volume/Å ³	1633.8(5)
Z	4
$\rho_{\text{calc}}/\text{g cm}^{-3}$	1.936
μ/mm^{-1}	0.177
F(000)	968
CCDC number	1510982

Figures S3 to S6

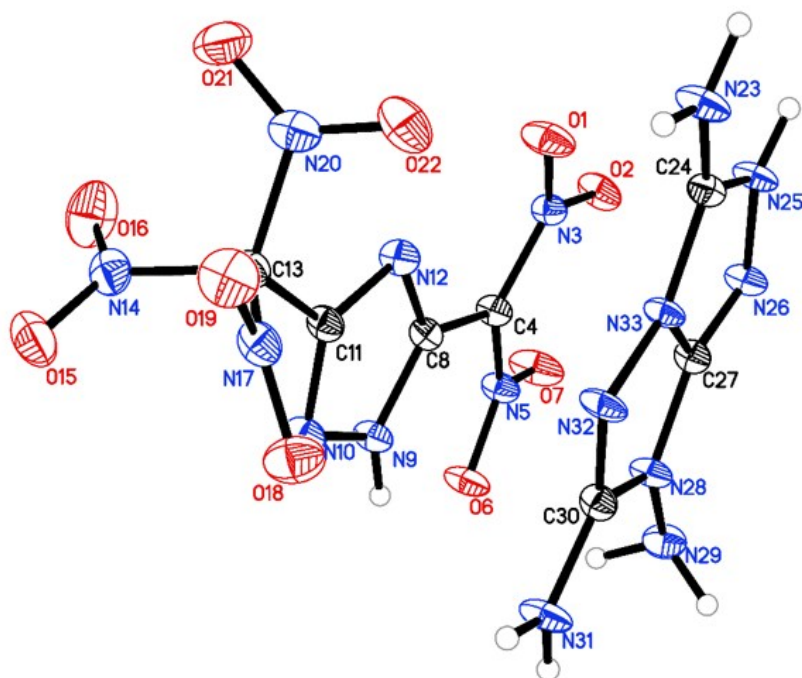


Figure S3. Single-crystal X-ray structures of **8** with numbering.

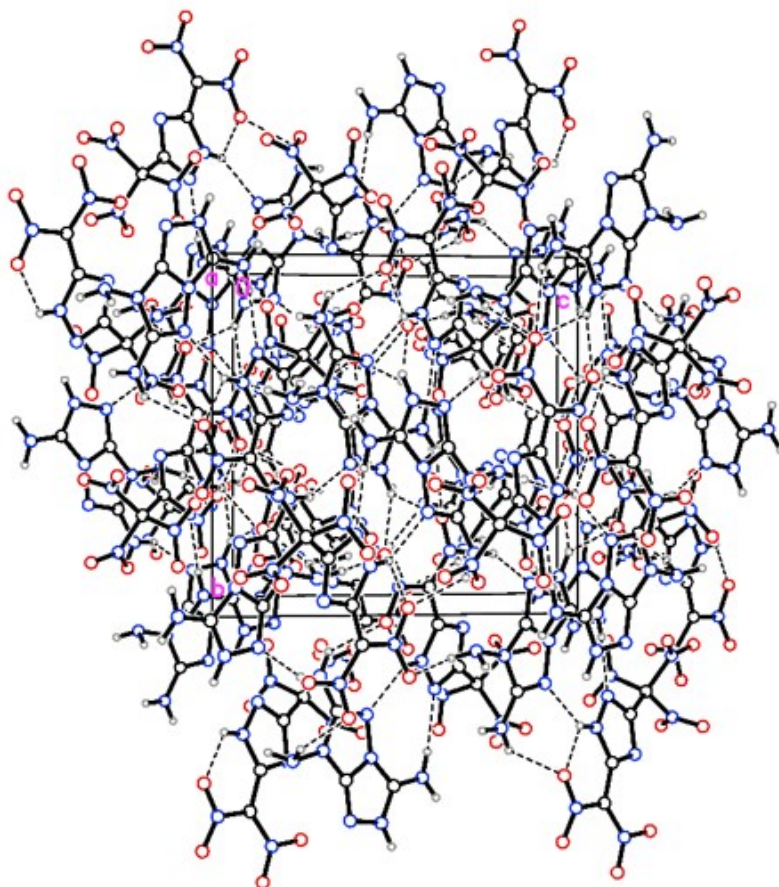


Figure S4. Unit cell view for **8** along *a* axis, hydrogen bonds are marked as dotted lines.

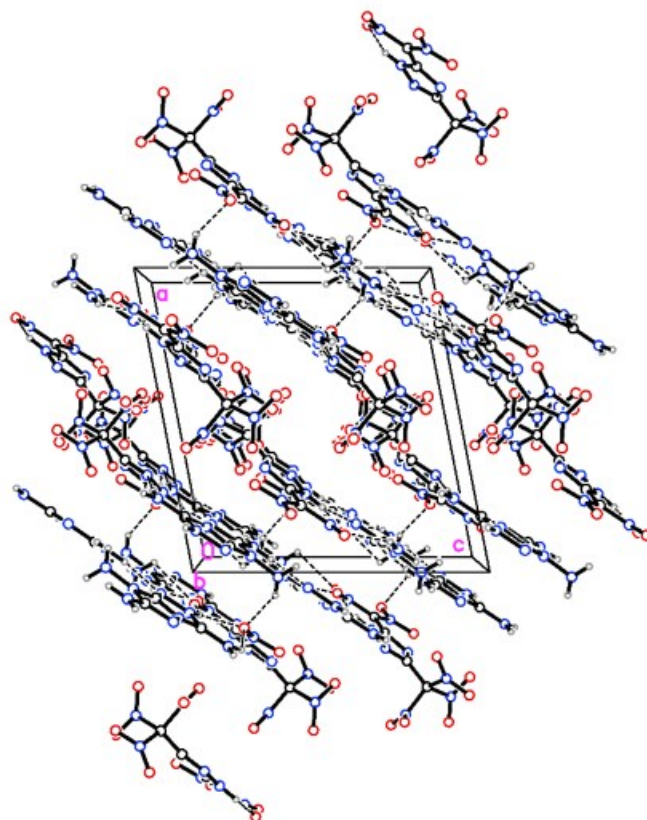


Figure S5. Unit cell view for **8** along *b* axis, hydrogen bonds are marked as dotted lines.

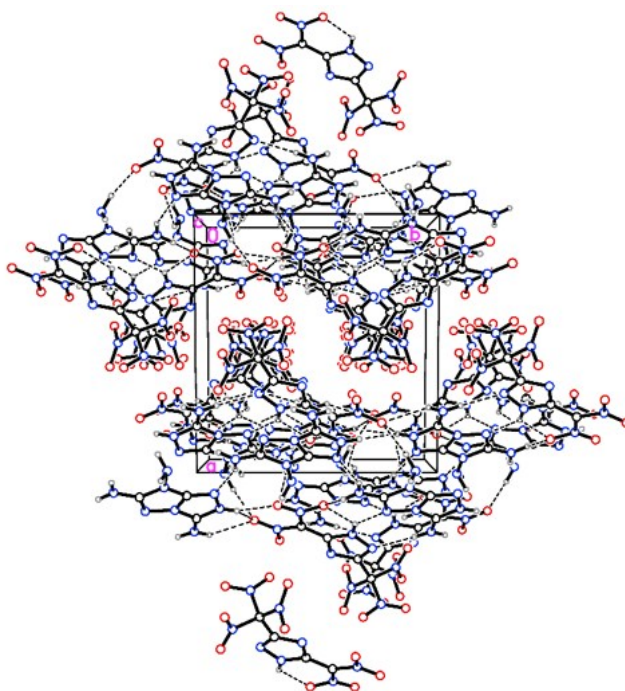


Figure S6. Unit cell view for **8** along *c* axis, hydrogen bonds are marked as dotted lines.

Table S2. Hydrogen bonds for **8** [Å and °]

D-H...A	d(D-H)	d(H...A)	d(D...A)	<(DHA)
N(31)-H(31A)...O(6)#2	0.88	2.20	2.922(2)	139.6
N(31)-H(31B)...N(26)#1	0.88	2.22	3.032(2)	153.4
N(29)-H(29B)...O(2)#1	0.88(2)	2.19(2)	2.996(2)	151.3(18)
N(9)-H(9)...N(32)#3	0.88	2.16	2.909(2)	143.4
N(9)-H(9)...O(6)	0.88	1.95	2.515(2)	120.2
N(23)-H(23B)...O(21)#4	0.88	2.55	3.278(2)	140.7
N(23)-H(23B)...O(2)#5	0.88	2.30	2.981(2)	133.7
N(23)-H(23A)...N(10)#2	0.88	2.14	3.015(2)	174.3
N(25)-H(25)...O(7)#5	0.88	2.01	2.764(2)	143.3
N(25)-H(25)...O(2)#5	0.88	2.05	2.773(2)	138.7

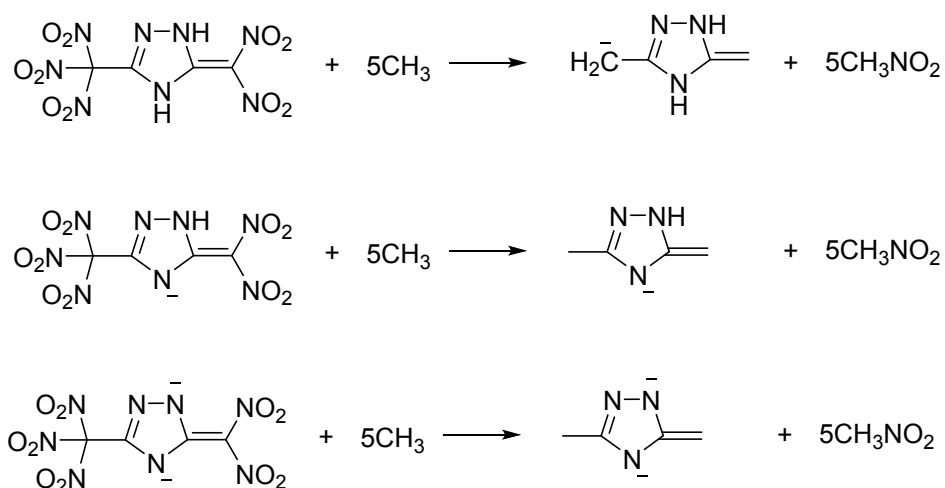
Symmetry transformations used to generate equivalent atoms:

#1 -x+2,y-1/2,-z+1/2 #2 x,-y+1/2,z+1/2 #3 x,-y+1/2,z-1/2

#4 -x+1,-y+1,-z+1 #5 x,-y+3/2,z+1/2

Theoretical calculations

As mentioned in the manuscript, the heats of formation for 5-(dinitromethyl)-3-(trinitromethyl)-*IH*-1,2,4-triazole as well as its monoanion and dianion were determined using isodesmic reactions (Scheme S1). The calculations were carried out using Gaussian 03 (Revision D.01) suite of programs.^[3] The geometric optimization and frequency analyses of the structures were calculated using B3LYP/6-31+G** level,^[10] and single energy points were calculated at the MP2/6-311++G** level.^[11] The heats of formation for the ammonium, the hydrazinium, guanidinium, and triaminoguanidinium ions were obtained by an atomization approach using G2 ab initio method^[12] (Table S3). The heat of formation for the 3,6,7-triamino-7H-[1,2,4]triazolo[4,3-b][1,2,4]triazol-2-ium ion was obtained from the literature.^[2] The heats of formation of other compounds in Scheme S2 were obtained from the NIST WebBook.^[13]



Scheme S1. Isodesmic reactions for calculating heats of formation for 5-(dinitromethyl)-3-(trinitromethyl)-1*H*-1,2,4-triazole as well as its monoanion and dianion.

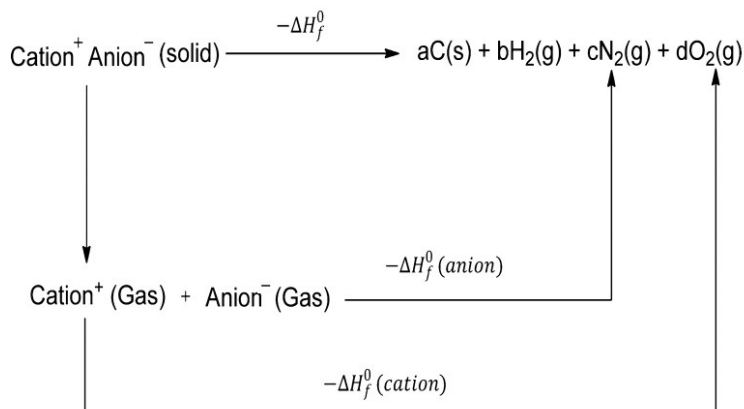
Table S3. Enthalpies of the gas-phase species.

M	ΔH_f° (kJ mol ⁻¹)
5-(dinitromethyl)-3-(trinitromethyl)-1 <i>H</i> -1,2,4-triazole	122.1
5-(dinitromethylene)-3-(trinitromethyl)-1,5-dihydro-1,2,4-triazol-4-ide	-146.4
5-(dinitromethylene)-3-(trinitromethyl)-1,2,4-triazole-1,4-diol	-29.2
ammonium ion	626.4
hydrazinium ion	770.0
3,6,7-triamino-7 <i>H</i> -[1,2,4]triazolo[4,3- <i>b</i>][1,2,4]triazol-2-ium	1090.6
guanidinium	575.9
triaminoguanidinium	883.6

The solid-state enthalpy of formation for a neutral compound can be estimated by subtracting the heat of sublimation from the gas-phase heat of formation. Based on the literature,^[14] the heat of sublimation can be estimated with Trouton's rule according to eq 1, where T represents either the melting point or the decomposition temperature when no melting occurs prior to decomposition:

$$\Delta H_{\text{sun}}^{\circ} = 188/\text{J mol}^{-1}\text{K}^{-1} * T_{\text{m(d)}} \quad (1)$$

For energetic salts, the solid-phase heat of formation is calculated on the basis of a Born-Haber energy cycle (Scheme S3).^[15] The number is simplified by equation 2:



Scheme S3. Born–Haber Cycle for the formation of energetic salts.

$$\Delta H_f^{\circ}(\text{salt}, 298 \text{ K}) = \Delta H_f^{\circ}(\text{cation}, 298\text{K}) + \Delta H_f^{\circ}(\text{anion}, 298\text{K}) - \Delta H_L \quad (2)$$

in which ΔH_L can be predicted by using the formula suggested by Jenkins, et al.^[15](equation 3):

$$\Delta H_L = U_{\text{pot}} + [p(n_M/2 - 2) + q(n_X/2 - 2)]RT \quad (3)$$

In this equation, n_M and n_X depend on the nature of the ions Mp^+ and Xq^- , respectively.

The equation for lattice potential energy U_{pot} (equation 4) has the form:^[15]

$$U_{\text{POT}} [\text{kJ mol}^{-1}] = \gamma(\rho_m/M_m)^{1/3} + \delta \quad (4)$$

where ρ_m [g cm^{-3}] is the density of the salt, M_m is the chemical formula mass of the ionic material, and values for γ ($\text{kJmol}^{-1}\text{cm}$) and δ (kJmol^{-1}) are assigned literature values.^[15] By using the measured room temperature densities, all the new compounds are listed in Table S4.

Table S4. Densities, calculated lattice energies, and calculated heats of formation of **6** **12**.

	$d^{[a]}$ [g cm ⁻³]	$\Delta_f H_{Lat}^{[b]}$ [kJ mol ⁻¹]	$\Delta_f H^{[c]}$ [kJ mol ⁻¹ /kJ g ⁻¹]
6	1.97	-	56.3/0.17
7	1.87	458.8	21.3/0.06
8	1.90	424.1	520.2/1.09
9	1.79	1224.1	286.7/0.70
10	1.65	1225.7	-2.1/-0.005
11	1.71	1146.0	-23.4/-0.05
12	1.73	1069.8	668.2/1.25

[a] Density - gas pycnometer at room temperature. [b] Calculated lattice energy. [c] Calculated heat of formation.

It has recently been found that an electrostatic potential (ESP) that is dominated by a positive region usually relates to a higher sensitivity towards mechanical stimulus.^[4] The positive regions of **6** was calculated at B3LYP/6-311+G(2d,p) optimized structure, and the 0.001 electron Bohr⁻³ isosurface of electron density is shown in Figure S7. The positive regions were found to concentrate at the dinitromethyl group and extend into the triazole ring, while the negative regions were mainly in the trinitromethyl group. Therefore, the atypical imbalance between positive regions and negative ones of **6** can result in higher sensitivity, which agrees with its experimental data.

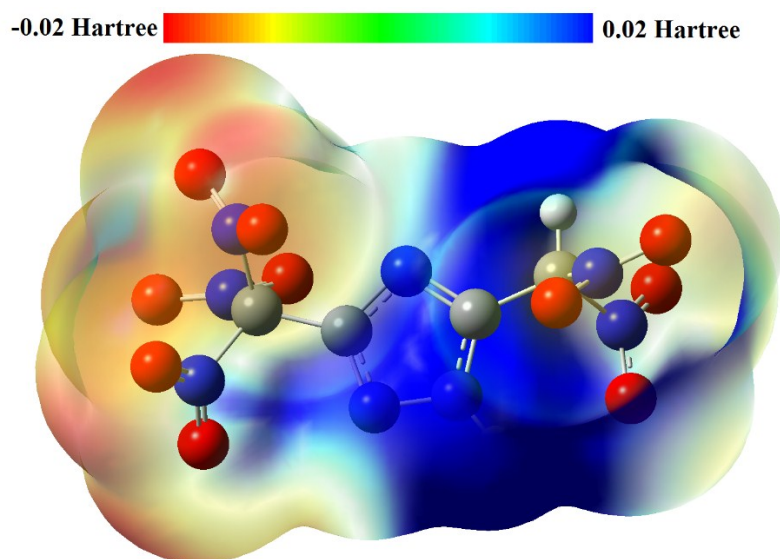


Figure S7. Electrostatic potential of **6** [B3LYP/6-311+G(2d,p), 0.001 electron/b³ isosurface, energy values -0.02 to +0.02 Hartree].

References

1. J. Zhang, S. Dharavath, L. A. Mitchell, D. A. Parrish, J. M. Shreeve, *J. Am. Chem. Soc.*, **2016**, *138*, 7500–7503.
2. Y. Ping, J. Zhang, D. A. Parrish, J. M. Shreeve, *J. Mater. Chem. A*, **2015**, *3*, 8606–8612.
3. M. J. Frisch, G. W. Trucks, H. G. Schlegel, G. E. Scuseria, M. A. Robb, J. A. Montgomery, T. V. Jr, K. N. Kudin, J. C. Burant, J. M. Millam, S. S. Iyengar, J. Tomasi, V. Barone, B. Mennucci, M. Cossi, G. Scalmani, N. Rega, G. A. Petersson, H. Nakatsuji, M. Hada, M. Ehara, K. Toyota, R. Fukuda, J. Hasegawa, M. Ishida, T. Nakajima, Y. Honda, O. Kitao, H. Nakai, M. Klene, X. Li, J. E. Knox, H. P. Hratchian, J. B. Cross, V. Bakken, C. Adamo, J. Jaramillo, R. Gomperts, R. E. Stratmann, O. Yazyev, A. J. Austin, R. Cammi, C. Pomelli, J. W. Ochterski, P. Y. Ayala, K. Morokuma, G. A. Voth, P. Salvador, J. J. Dannenberg, V. G. Zakrzewski, S. Dapprich, A. D. Daniels, M. C. Strain, O. Farkas, D. K. Malick, A. D. Rabuck, K. Raghavachari, J. B. Foresman, J. V. Ortiz, Q. Cui, A. G. Baboul, S. Clifford, J. Cioslowski, B. B. Stefanov, A. L. G. Liu, P. Piskorz, I. Komaromi, R. L. Martin, D. J. Fox, T. Keith, M. A. Al-Laham, C. Peng, A. Nanayakkara, M. Challacombe, P. M. W.

- Gill, B. Johnson, W. Chen, M. Wong, C. Gonzalez, J. A. Pople, *Gaussian 03*, Revision D.01. Gaussian, Inc.: Wallingford, CT, **2004**.
4. a) J. Zhang, Shreeve, *J. Am. Chem. Soc.* **2014**, *136*, 4437–4445; b) Y. Li, H. Gao, J. Zhang, S. Li, W. Zhou, *Magn. Reson. Chem.* **2012**, *50*, 16–21.
 5. Bruker. APEX2 v2010.3-0. Bruker AXS Inc., Madison, Wisconsin, USA, **2014**.
 6. Bruker. SAINT v7.68A. Bruker AXS Inc., Madison, Wisconsin, USA, **2009**.
 7. Bruker. XPREP v2008/2. Bruker AXS Inc., Madison, Wisconsin, USA, **2014**.
 8. Bruker. SADABS v2008/1, Bruker AXS Inc., Madison, Wisconsin, USA, **2008**.
 9. G. M. Sheldrick, SHELXL-2014/7. University of Göttingen, Germany, **2014**; b) L. Farrugia, *J. Appl. Cryst.* **2012**, *45*, 849–854.
 10. R. G. Parr, W. Yang, *Density Functional Theory of Atoms and Molecules*, Oxford University Press, New York, **1989**.
 11. M. Head-Gordon, J. A. Pople, *Chem. Phys. Lett.* **1988**, *153*, 503–506.
 12. J. M. Martin, *Chem. Phys. Lett.* **1996**, *259*, 669–678.
 13. P. J. Linstrom, W. G. Mallard, Eds. NIST Chemistry WebBook, NIST Standard Reference Database, 69, National Institute of Standards and Technology, **2005**.
 14. a) F. Trouton, *Philos. Mag.* **1884**, *18*, 54–57; b) M. S. Westwell, M. S. Searle, D. J. Wales, D. H. Williams, *J. Am. Chem. Soc.* **1995**, *117*, 5013–5015.
 15. H. D. B. Jenkins, D. Tudela, L. Glasser, *Inorg. Chem.* **2002**, *41*, 2364–2367.